

RESEARCH

Open Access



Detection and performance analysis for MIMO visible light communication system using joint optical spatial and pulse amplitude width modulation

Wei-Chiang Wu^{1*}

*Correspondence:
lclunds@163.com

¹ School of Mechanical and Electrical Engineering, Sanming University, No. 25 Jingdong Rd., Sanming, Fujian, China

Abstract

Conventional optical spatial modulation (SM) scheme activates one of the light-emitting diodes (LEDs) to transmit an intensity-modulated optical signal, in which the index of the activated LED is determined by spatial symbol and the emitted intensity is controlled by temporal symbol. In order to enhance the spectral efficiency (bits per channel use), we propose a joint SM and pulse amplitude width modulation (PAWM) as a novel optical spatial-temporal signaling scheme. In this paper, the proposed SM-PAWM optical signaling scheme is applied in a multi-input multi-output (MIMO) visible light communication (VLC) system. Employing optimal maximum likelihood (ML) algorithm to extract the spatial and temporal symbols is computationally prohibitive; hence, we develop a novel low-complexity detection scheme that converts the joint optimization problem separately to decode the spatial and temporal symbols. Moreover, theoretical results in terms of the successful identification probability of activated LED as well as the overall symbol error rate are derived. Extensive computer simulations are performed to validate the analytical results. It is shown that the proposed detection scheme is a feasible alternative to the ML detector in the VLC-MIMO system employing SM-PAWM.

Keywords: Spatial modulation (SM), Multi-input multi-output (MIMO), Visible light communication (VLC), Spatial matched filtering (SMF), Pulse amplitude width modulation (PAWM)

1 Introduction

Spatial modulation (SM) is a new promising MIMO technology that carries the information simultaneously over both the spatial and temporal domains [1–5]. Compared with conventional MIMO scheme, SM avoids the Inter-Channel Interference (ICI), requires no Inter-Antennas Synchronization (IAS), and needs one or only a few RF chains for data transmission. Hence, low-complexity implementation can be achieved in SM MIMO scheme. Moreover, one of the major advantages of SM is the increase in bits per channel use (bpcu) by a factor equal to the logarithm of the number of antennas at the transmitter. Recently, it has also been shown that SM technique can be applied

for optical wireless communication systems [6–10], particularly for indoor visible light communication (VLC) system. The reason is due mainly to the static and line-of-sight (LoS) characteristic of indoor VLC channel. Therefore, the location-dependent spatial constellation is plausible to be further utilized to boost the overall spectral efficiency [11–15].

In optical space-shift keying (SSK) [6], the input bits are used to select only single laser source or light-emitting diode (LED) while the rest are idle to send an optical pulse over an indoor channel at each transmission instant. In the work of [16], optical generalized space shift keying (GSSK) is proposed and analyzed in which multiple LEDs are activated simultaneously. Notice that no temporal modulated symbol is transmitted by the activated LED for SSK or GSSK. To increase the bpcu, the transmitted bits stream of the SM scheme is composed of two information-carrying blocks, in terms of spatial and temporal symbols. Like SSK scheme, spatial symbol determines one from the array of LED at the transmitter. The chosen LED is obliged for temporal data transmission. In the scheme proposed in [9], the temporal symbol is mapped to the pulse position modulation (PPM) signal constellation diagram, which is named spatial pulse position modulation (SPPM), *e.g.*, a single PPM symbol is sent from an active transmit antenna at each signaling period, while in the work of [10], SM employing pulse amplitude modulation (PAM) is shown to outperform repetition coding (RC) when high spectral efficiencies are desired. SM (GSM) technique in which an unipolar M -ary PAM (MPAM) optical signal is transmitted by the active LEDs at each time instance is applied for MIMO VLC system [12, 15, 17, 18].

To further achieve a higher spectral efficiency in optical SM systems, we joint use of multiple optical pulse amplitudes as well as widths for temporal symbol modulation. Hence, we propose a novel optical SM system, denoted as a (N_t, M, N) -ary spatial pulse amplitude width modulation (SM-PAWM). We apply the SM-PAWM scheme in a VLC MIMO system. Most past works for optical SM scheme employs maximum likelihood (ML) decision rule to jointly demodulate the temporal and spatial symbols. However, since ML detection requires exhaustive searches on the parameters embedded in the SM-PAWM signal, the computation load is prohibitive in general scenario. For this reason, one of the contributions of this paper is to propose a novel low-complexity detection scheme. Rather than jointly optimization, the received vector signal at the output of photodetectors (PDs) is first linearly transformed by spatial matched filtering (SMF). Since the optical PAWM signal is intensity modulated and channel vector is location dependent, hence, energy detection is utilized at the output of SMF to identify the index of the active LED. In what follows, the (M, N) -ary PAWM signal is then demodulated separately by M -ary PAM and N -ary pulse width modulation (PWM) multi-levels circuits with modified minimum distance between the signal constellation points. Performance in terms of the average overall symbol error rate (SER) is extensively analyzed. All theoretical derivations are validated by Monte Carlo simulations which are in good agreement.

Major contributions of this work are summarized as follows:

- (1) We propose a novel (N_t, M, N) -ary SM-PAWM spatial–temporal modulation and demodulation scheme that increases the bpcu of conventional SM.

- (2) Typical ML-based receiver relies on joint optimization of multiple parameters. We propose a simple detection algorithm that separates the joint optimization into individually sequential optimization problems.
- (3) The overall average SER of the proposed detection scheme is comprehensively analyzed. We first derive the spatial domain SER, *i.e.*, the probability of misidentifying the index of the active LED. There then, we devise the (M, N) -ary PAWM temporal domain SER given that the index of active LED has been correctly identified. Based on the two probabilities, the theoretical expression of the overall average SER is derived.
- (4) Extensive computer simulations are performed to demonstrate the analytical results.

Notation: We use upper and lower case boldface letters to denote matrices and vectors, respectively. $[\cdot]^T, [\cdot]^H$ stand for matrix or vector transpose and complex transpose, respectively. $\|\mathbf{a}\|$ denotes the l_2 -norm of vector \mathbf{a} . We use $E\{\cdot\}$ for expectation (ensemble average). \mathbf{I}_K denotes an identity matrix of size K . \mathbf{e}_k^L denotes the k th column vector of an identity matrix of size L . A Gaussian distributed random variable with mean μ variance σ^2 reads as $N(\mu, \sigma^2)$. \hat{x} means the estimate of x . $\mathbf{x}(i)$ denotes the i th element of vector \mathbf{x} . $\mathbf{A}|_{(i,j)}$ denotes the element of the i th row and j th column of matrix \mathbf{A} . $\text{tr}(\mathbf{V})$ denotes the trace of matrix \mathbf{V} . $\|\mathbf{C}\|_F^2$ means the Frobenius norm of matrix \mathbf{C} . The tail function reads as $Q(x) \equiv \frac{1}{\sqrt{2\pi}} \int_x^\infty \exp\left(-\frac{t^2}{2}\right) dt$.

2 Methods/experimental

2.1 Channel model

In this work, we consider a VLC indoor line-of-sight (LoS) MIMO channel [19, 20], in which N_t LEDs are deployed at the transmitter and N_r PDs are equipped at the receiving front end. A schematic illustration of the system is depicted in Fig. 1, where the dashed lines represent the LEDs are active and the solid lines denote the LEDs are inactive to every receiving PDs at user terminal. In VLC channel, only the (dominant) component of the channel gain is considered. The MIMO channel with dimension $N_r \times N_t$ considered in this paper is

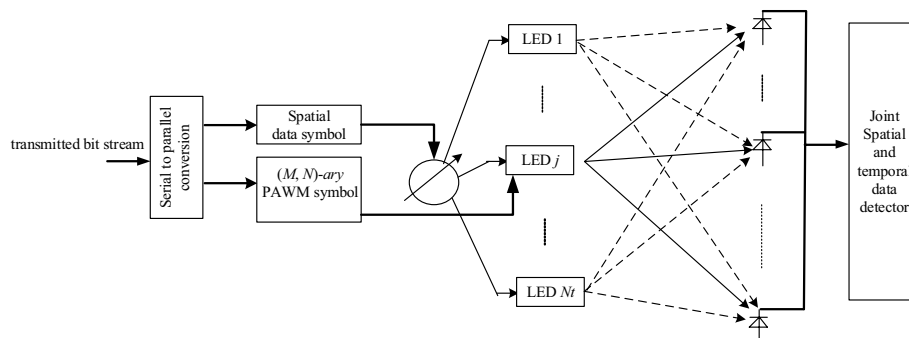


Fig. 1 Block diagram of the VLC system using GSM

$$\mathbf{H} = \begin{bmatrix} h_{11} & h_{12} & \dots & h_{1N_t} \\ h_{21} & h_{22} & \dots & h_{2N_t} \\ \dots & \dots & \dots & \dots \\ h_{N_r1} & h_{N_r2} & \dots & h_{N_rN_t} \end{bmatrix}_{N_r \times N_t} = [\mathbf{h}_1 \ \mathbf{h}_2 \ \dots \ \mathbf{h}_{N_t}] \tag{1}$$

where $\mathbf{h}_i = [h_{1i} \ h_{2i} \ \dots \ h_{N_r i}]^T$ denotes the $N_r \times 1$ channel vector seen by the array of PDs as signal is emitted from the i th LED. h_{ij} represents the channel gain of the VLC link between the j th LED and the i th PD in indoor LoS environment. We adopt the channel model as suggested in [21]

$$h_{ij} = \begin{cases} \frac{\eta(k+1)A}{2\pi d_{ij}^2} \cos^k(\phi_{ij}) \cos(\varphi_{ij}); & 0 \leq \varphi_{ij} \leq \Psi_{1/2} \\ 0; & \varphi_{ij} > \Psi_{1/2} \end{cases} \tag{2}$$

where k is the Lambertian emission order given as $k = -\frac{\ln 2}{\ln(\cos \phi_{1/2})}$, $\phi_{1/2}$ is the semi-angle at half-power of the LED, d_{ij} is the transmission distance between the j th LED and the i th PD, ϕ_{ij} and φ_{ij} are the angle of emission and incidence from the j th LED to the i th PD. A , η and $\Psi_{1/2}$ represent the PD physical area, PD responsivity and half-power field-of-view (FOV) angle of the PD, respectively.

2.2 Signal model

As shown in Fig. 1, the bit stream of the proposed SM based PAWM scheme is divided into two blocks at each transmission time interval: The first block of bit stream with length k , $[b_1 \ b_2 \ \dots \ b_k]$, is referred to as “spatial symbol.” The spatial symbol is used to activate a particular LED, while the other $(N_t - 1)$ LEDs are kept silent. The second block of bit stream with length $l + q$, $[b_{k+1} \ b_{k+2} \ \dots \ b_{k+l}, \ b_{k+l+1} \ b_{k+l+2} \ \dots \ b_{k+l+q}]$, is referred to as “temporal symbol.” According to the nature of optical signals, intensity modulation and direct detection are usually employed. A PWM waveform consists of a sequence of pulses with each pulse having a width proportional to the symbol to be transmitted. Likewise, a PAM waveform consists of a sequence of pulses with each pulse having an amplitude proportional to the symbol to be transmitted. In this paper, the optical pulses with pulse width $n\tau$; $n \in \{1, \dots, N\}$ and amplitude $\frac{mP_t}{M}$; $m \in \{1, \dots, M\}$ are used to represent the N -ary PWM (NPWM) and M -ary PAM (MPAM) signals, respectively. P_t is the optical emission intensity of the activated LED, m is determined by the first l -bits subblock, $[b_{k+1} \ b_{k+2} \ \dots \ b_{k+l}]$, while n is determined by the second q -bits subblock, $[b_{k+l+1} \ b_{k+l+2} \ \dots \ b_{k+l+q}]$. $M = 2^l$ and $N = 2^q$. Hence, the optical signal to be transmitted by the active LED belongs to a two-dimensional (M, N) -ary PAWM alphabet. An example of $(2, 4)$ -ary PAWM transmitted pulse waveform is depicted in Fig. 2.

The spectral efficiency (measured by bpcu) of SM-PAWM scheme can be calculated as

$$\eta = \log_2 N_t + \log_2 M + \log_2 N = (k + l + q) \text{ bpcu} \tag{3}$$

Define the rectangular function with unit height and width τ as

$$p_\tau(t) = \begin{cases} 1; & 0 \leq t < \tau \\ 0; & \text{elsewhere} \end{cases} \tag{4}$$

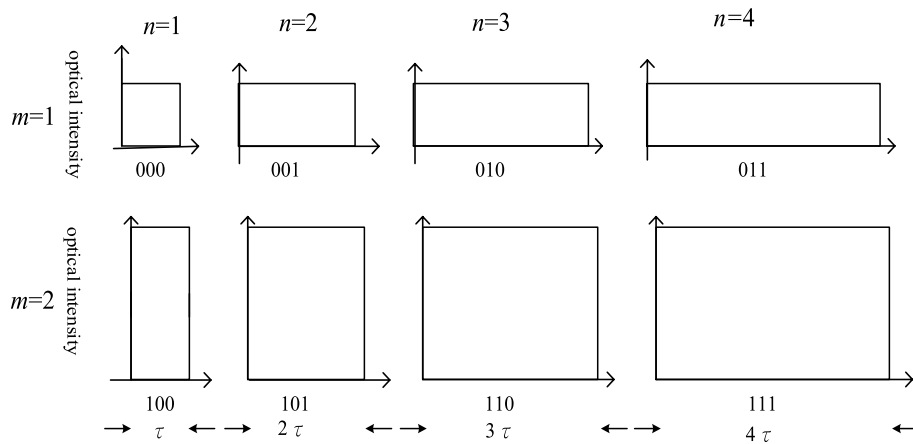


Fig. 2 (2, 4)-ary PAWM transmitted pulse waveforms

Then the PAWM temporal symbol carried by the active LED can be expressed as

$$s_{m,n}(t) = \frac{mP_t}{M} p_{n\tau}(t); 0 \leq t \leq N\tau, m \in \{1, \dots, M\}, n \in \{1, \dots, N\} \tag{5}$$

3 Detection algorithm description

As shown in Fig. 1, at the front end of the receiver, N_r PDs receive the optical PAWM signal and convert them into electrical signals. If the u th LED is activated and the temporal signal $s_{m,n}(t)$ is emitted, then the received $N_r \times 1$ vector can be written as

$$\begin{aligned} \mathbf{r}(t) &= \mathbf{H}\mathbf{x}_{m,n,u}(t) + \mathbf{v}(t) \\ &= \mathbf{H}\mathbf{e}_u^{N_t} s_{m,n}(t) + \mathbf{v}(t); 0 \leq t \leq N\tau \\ &= \mathbf{h}_u s_{m,n}(t) + \mathbf{v}(t) \end{aligned} \tag{6}$$

where \mathbf{H} is the MIMO channel matrix as defined in (1). $\mathbf{x}_{m,n,u}(t) = [0 \dots 0 s_{m,n}(t) 0 \dots 0]^T$ is the N_t -dimensional vector with single non-zero element at the u th element, which is $s_{m,n}(t)$. $\mathbf{e}_u^{N_t}$ is the u th column vector of N_t -dimensional identity matrix. Each element in $\mathbf{v}(t)$ represents the sum of the thermal noise and the high intensity ambient light shot noise at the PD. We model each element in $\mathbf{v}(t)$ as independent and identically distributed real valued additive white Gaussian noise (AWGN) having zero mean and power spectral density σ^2 .

Integrating the received signal within $t \in [(j-1)\tau, j\tau]; j = 1, \dots, N$ and defining $\mathbf{r}_j \equiv \int_{(j-1)\tau}^{j\tau} \mathbf{r}(t) dt, \mathbf{v}_j \equiv \int_{(j-1)\tau}^{j\tau} \mathbf{v}(t) dt$, then we may convert (6) into matrix form

$$\mathbf{R} = \mathbf{H}\mathbf{X}_{m,n,u} + \mathbf{V} \tag{7}$$

where $\mathbf{R}, \mathbf{V} \in \mathbb{R}^{N_r \times N}, \mathbf{X}_{m,n,u} \in \mathbb{R}^{N_t \times N}, \mathbf{R} \equiv [\mathbf{r}_1 \mathbf{r}_2 \dots \mathbf{r}_N], \mathbf{V} \equiv [\mathbf{v}_1 \mathbf{v}_2 \dots \mathbf{v}_N]$. Since

$$\int_{(j-1)\tau}^{j\tau} s_{m,n}(t) dt = \int_{(j-1)\tau}^{j\tau} \frac{mP_t}{M} p_{n\tau}(t) dt = \begin{cases} \frac{mP_t}{M} \tau; & \text{if } j \leq n \\ 0; & \text{if } j > n \end{cases} \tag{8}$$

There then, the observation matrix can be rewritten as

$$\mathbf{R} = \frac{mP_t}{M} \tau \mathbf{h}_u [\underbrace{1 \dots 1}_{n \text{ elements}} \quad \underbrace{0 \dots 0}_{N-n \text{ elements}}] + \mathbf{V} \tag{9}$$

Based on the assumption that channel state information (CSI) is available at the receiver, we aim to estimate the index of the active LED and demodulate the (M, N) -ary PAWM temporal symbol carried by the activated LED.

3.1 Maximum likelihood (ML) detection

Assuming equal a priori probability for both spatial and temporal symbols, the *maximum* a posteriori (MAP) decision rule is equivalent to the maximum likelihood (ML) criterion. Under AWGN, the ML detector computes the Euclidean distance between the received vector signal, $\mathbf{r}(t)$, and the set of all possible received signals, and selects the minimum one. Based on (7), the active LED indices and the corresponding (M, N) -ary PAWM temporal symbol carried by the activated LED can be extracted by

$$\begin{aligned} (\hat{m}, \hat{n}, \hat{u}) &= \arg \max_{m,n,u} f(\mathbf{r}(t) | \mathbf{H}) \\ &= \arg \min_{m,n,u} \|\mathbf{R} - \mathbf{H}\mathbf{X}_{m,n,u}\|_F^2 \\ &= \arg \min_{m,n,u} \left\| \mathbf{R} - \frac{mP_t}{M} \tau \mathbf{h}_u [\underbrace{1 \dots 1}_{n \text{ elements}} \quad \underbrace{0 \dots 0}_{N-n \text{ elements}}] \right\|_F^2 \end{aligned} \tag{10}$$

The ML detection procedure requires the joint exhausting searches over all the possible sets of the activated LEDs as well as all the possible (M, N) -ary PAWM constellation-point sets, *e.g.*, to perform (10), it requires MNN_t trials. The load of computations required to implement (10) is to be evaluated in Sect. 5.1.

3.2 Proposed detection scheme

3.2.1 Spatial symbol detection algorithm

To make the detector feasible, we separate the joint optimization problem of (10) into sequential detection processes. The schematic diagram of the proposed detector is shown

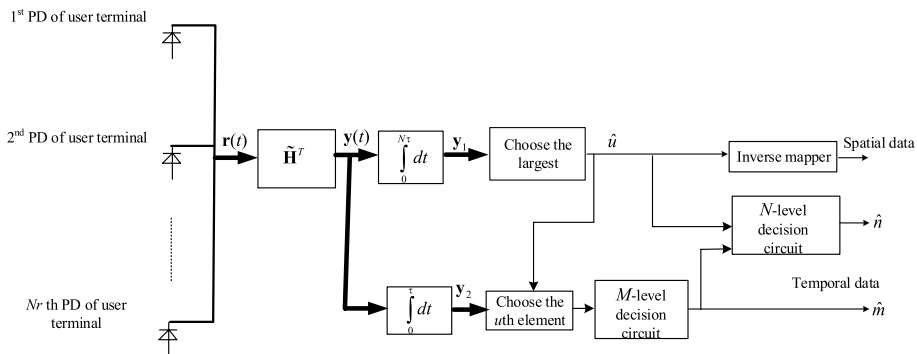


Fig. 3 Block diagram of the proposed SM-PAWM detector in VLC MIMO system

in Fig. 3. As shown in Fig. 3, the observation vector $\mathbf{r}(t)$ is first sent to a bank of N_t spatial MF (SMF) that matches to the spatial signature vector of each LED. Let the normalized $N_r \times 1$ channel vector be defined as $\tilde{\mathbf{h}}_i = \frac{\mathbf{h}_i}{\|\mathbf{h}_i\|}$, $i = 1, \dots, N_t$, then the weight vector of each of the SMF is designed as

$$\mathbf{w}_{j, MF} = \tilde{\mathbf{h}}_j; j = 1, \dots, N_t \tag{11}$$

Upon defining $\mathbf{W} \equiv [\mathbf{w}_{1, MF} \ \mathbf{w}_{2, MF} \ \dots \ \mathbf{w}_{N_t, MF}] = [\tilde{\mathbf{h}}_1 \ \tilde{\mathbf{h}}_2 \ \dots \ \tilde{\mathbf{h}}_{N_t}]$, then the outputs of N_t spatial SMFs are $\mathbf{y}(t) = \mathbf{W}^T \mathbf{r}(t)$. Let the correlation between k th and j th normalized channel vectors be defined as $\alpha_{kj} = (\tilde{\mathbf{h}}_k)^T \tilde{\mathbf{h}}_j$, hence we have

$$\begin{aligned} \mathbf{W}^T \mathbf{h}_u &= [\tilde{\mathbf{h}}_1 \ \tilde{\mathbf{h}}_2 \ \dots \ \tilde{\mathbf{h}}_{N_t}]^T \tilde{\mathbf{h}}_u \|\mathbf{h}_u\| \\ &= \begin{bmatrix} \alpha_{1u} \\ \alpha_{2u} \\ \vdots \\ 1 \\ \vdots \\ \alpha_{N_t u} \end{bmatrix} \|\mathbf{h}_u\| = \boldsymbol{\alpha}_u \|\mathbf{h}_u\| \end{aligned} \tag{12}$$

where $\boldsymbol{\alpha}_u \equiv [\alpha_{1u} \ \alpha_{2u} \ \dots \ 1 \ \dots \ \alpha_{N_t u}]^T$ is the u th column vector of $\mathbf{W}^T \mathbf{W}$ in which the u th element of $\boldsymbol{\alpha}_u$ being 1. Giving that the u th LED is activated and the temporal PAWM signal $s_{m,n}(t)$ is emitted, i.e., $\mathbf{r}(t) = \mathbf{h}_u s_{m,n}(t) + \mathbf{v}(t)$, then the $N_t \times 1$ SMF output vector can be obtained as

$$\mathbf{y}(t) = \mathbf{W}^T \mathbf{h}_u s_{m,n}(t) + \mathbf{W}^T \mathbf{v}(t) = \boldsymbol{\alpha}_u \|\mathbf{h}_u\| s_{m,n}(t) + \tilde{\mathbf{v}}(t); \quad ; 0 \leq t \leq N\tau \tag{13}$$

where $\tilde{\mathbf{v}}(t) \equiv \mathbf{W}^T \mathbf{v}(t)$. To collect the energy in temporal domain within the observation interval, we integrate the output of each SMF over $N\tau$, which yields

$$\mathbf{y}_1 \equiv \int_0^{N\tau} \mathbf{y}(t) dt = \boldsymbol{\alpha}_u \|\mathbf{h}_u\| \int_0^{N\tau} s_{m,n}(t) dt + \int_0^{N\tau} \tilde{\mathbf{v}}(t) dt \tag{14}$$

Since $\int_0^{N\tau} s_{m,n}(t) dt = \int_0^{N\tau} \frac{mP_t}{M} p_{n\tau}(t) dt = \frac{P_t m n \tau}{M}$, and let $\tilde{\mathbf{v}}_1 \equiv \int_0^{N\tau} \tilde{\mathbf{v}}(t) dt$, then (14) can be reformulated as

$$\mathbf{y}_1 = \frac{\|\mathbf{h}_u\| P_t m n \tau}{M} \boldsymbol{\alpha}_u + \tilde{\mathbf{v}}_1 \tag{15}$$

In what follows, the u th element of \mathbf{y}_1 is

$$\mathbf{y}_1(u) = \begin{cases} \frac{\|\mathbf{h}_u\| P_t m n \tau}{M} + \tilde{\mathbf{v}}_1(u); & \text{if the } u\text{th LED is activated} \\ \frac{\alpha_{ku} \|\mathbf{h}_k\| P_t m n \tau}{M} + \tilde{\mathbf{v}}_1(u); & \text{if the } k\text{th LED is activated, } k \neq u \end{cases}$$

It is evident that $\tilde{\mathbf{v}}_1$ is still Gaussian with zero-mean and covariance matrix

$$\begin{aligned}
 \mathbf{C}_1 &= E\{\tilde{\mathbf{v}}_1\tilde{\mathbf{v}}_1^T\} = E\left\{\int_0^{N\tau}\tilde{\mathbf{v}}(t)dt\int_0^{N\tau}\tilde{\mathbf{v}}^T(\lambda)d\lambda\right\} = E\left\{\int_0^{N\tau}\mathbf{W}^T\mathbf{v}(t)dt\int_0^{N\tau}\mathbf{v}^T(\lambda)\mathbf{W}d\lambda\right\} \\
 &= \int_0^{N\tau}\int_0^{N\tau}\mathbf{W}^TE\{\mathbf{v}(t)\mathbf{v}^T(\lambda)\}\mathbf{W}d\lambda dt = \sigma^2\int_0^{N\tau}\int_0^{N\tau}\mathbf{W}^T\delta(t-\lambda)\mathbf{I}_{N_r}\mathbf{W}d\lambda dt \\
 &= \sigma^2\mathbf{W}^T\mathbf{W}\int_0^{N\tau}dt = \sigma^2N\tau\mathbf{W}^T\mathbf{W}
 \end{aligned} \tag{16}$$

As depicted in (16), the noise term $\tilde{\mathbf{v}}_1(u)$ is a Gaussian random variable with zero-mean and variance $\sigma^2N\tau$.

In the considered SM-PAWM scheme, only single LED is activated during the observation interval and the optical signal is intensity modulated. Hence, as depicted in Fig. 3, the index of active LED is determined by choosing the largest among the outputs of N_t SMFs. The spatial information bits, $[b_1 b_2 \dots b_k]$, can then be decoded by the following SM inverse mapper.

3.2.2 (M, N)-ary PAWM temporal symbol detection algorithm

As shown in Fig. 3, to demodulate the M -ary PAM (MPAM) symbol, we integrate the output of each SMF over $t \in [0, \tau]$, which yields

$$\mathbf{y}_2 \equiv \int_0^\tau \mathbf{y}(t)dt = \boldsymbol{\alpha}_u\|\mathbf{h}_u\|\int_0^\tau s_{m,n}(t)dt + \int_0^\tau \tilde{\mathbf{v}}(t)dt \tag{17}$$

Since $\int_0^\tau s_{m,n}(t)dt = \int_0^\tau \frac{mP_t}{M}p_{nr}(t)dt = \frac{P_tm\tau}{M}$, and let $\tilde{\mathbf{v}}_2 \equiv \int_0^\tau \tilde{\mathbf{v}}(t)dt$, then we arrive at

$$\mathbf{y}_2 = \frac{\|\mathbf{h}_u\|P_tm\tau}{M}\boldsymbol{\alpha}_u + \tilde{\mathbf{v}}_2 \tag{18}$$

Similar to the derivation of (16), we have that $\tilde{\mathbf{v}}_2$ is still Gaussian with zero-mean and covariance matrix

$$\begin{aligned}
 \mathbf{C}_2 &= E\{\tilde{\mathbf{v}}_2\tilde{\mathbf{v}}_2^T\} = E\left\{\int_0^\tau\tilde{\mathbf{v}}(t)dt\int_0^\tau\tilde{\mathbf{v}}^T(\lambda)d\lambda\right\} = \int_0^\tau\int_0^\tau\mathbf{W}^TE\{\mathbf{v}(t)\mathbf{v}^T(\lambda)\}\mathbf{W}d\lambda dt \\
 &= \sigma^2\mathbf{W}^T\mathbf{W}\int_0^\tau dt = \sigma^2\tau\mathbf{W}^T\mathbf{W}
 \end{aligned} \tag{19}$$

As depicted in (18), the u th element of \mathbf{y}_2 is

$$\begin{aligned}
 y_2(u) &= \frac{\|\mathbf{h}_u\|P_tm\tau}{M} + \tilde{v}_2(u); \quad m \in \{1, \dots, M\} \\
 &= md_{u,2} + \tilde{v}_2(u)
 \end{aligned} \tag{20}$$

It is evident from (20) that given the u th LED is active, the distance between M -ary PAM adjacent signal constellation points is

$$d_{u,2} = \frac{\|\mathbf{h}_u\|P_t\tau}{M} \tag{21}$$

Under AWGN and equal a priori probability, the optimum M -ary PAM demodulator is a multi-level decision circuit according to the following decision rule.

$$\text{decide} \begin{cases} \hat{m} = 1; & \text{if } \mathbf{y}_2(u) < \frac{3}{2}d_{u,2} \\ \vdots \\ \hat{m} = l; & \text{if } \frac{(2l-1)d_{u,2}}{2} < \mathbf{y}_2(u) < \frac{(2l+1)d_{u,2}}{2} \\ \vdots \\ \hat{m} = M; & \text{if } \frac{(2M-1)d_{u,2}}{2} < \mathbf{y}_2(u) \end{cases} \tag{22}$$

As derived in (15), given that the u th LED is active, the u th element of \mathbf{y}_1 is

$$\mathbf{y}_1(u) = \frac{\|\mathbf{h}_u\|P_t m n \tau}{M} + \tilde{\mathbf{v}}_1(u) \tag{23}$$

As shown in Fig. 3, to demodulate the N -ary PWM (NPWM) symbol, the information of \hat{m} obtained from (22) should be exploited. Therefore, the spacing between any two adjacent NPWM constellation points at the u th element of \mathbf{y}_1 is

$$d_{u,1} = \frac{\|\mathbf{h}_u\|P_t \hat{m} \tau}{M} \tag{24}$$

Substituting (24) into (23), we have

$$\mathbf{y}_1(u) = n d_{u,1} + \tilde{\mathbf{v}}_1(u) \tag{25}$$

There then, a multi-level decision circuit with the following decision rule can be implemented to demodulate the N -ary PWM symbol.

$$\text{decide} \begin{cases} \hat{n} = 1; & \text{if } \mathbf{y}_1(u) < \frac{3}{2}d_{u,1} \\ \vdots \\ \hat{n} = l; & \text{if } \frac{(2l-1)d_{u,1}}{2} < \mathbf{y}_1(u) < \frac{(2l+1)d_{u,1}}{2} \\ \vdots \\ \hat{n} = N; & \text{if } \frac{(2N-1)d_{u,1}}{2} < \mathbf{y}_1(u) \end{cases} \tag{26}$$

4 Average symbol error rate (SER) analysis

4.1 SER of the ML detector

In general, deriving the exact SER of the optimum ML detector is intractable. Nevertheless, the union bound technique can be applied to express the upper bound of the average SER of a point to point optical SM MIMO VLS system as

$$P_{e,ML} \leq \frac{1}{2N_t M N} \sum_{u=1}^{N_t} \sum_{\hat{u}=1}^{N_t} \sum_{m=1}^M \sum_{\hat{m}=1}^M \sum_{n=1}^N \sum_{\hat{n}=1}^N P_e(\mathbf{x}_{m,n,u}(t) \rightarrow \mathbf{x}_{\hat{m},\hat{n},\hat{u}}(t)) \tag{27}$$

$(u,m,n) \neq (\hat{u},\hat{m},\hat{n})$

where $P_e(\mathbf{x}_{m,n,u}(t) \rightarrow \mathbf{x}_{\hat{m},\hat{n},\hat{u}}(t))$ denotes the pairwise error probability (PEP) of transmitting $\mathbf{x}_{m,n,u}(t)$ and detecting erroneously as $\mathbf{x}_{\hat{m},\hat{n},\hat{u}}(t)$. The event of a symbol error occurs in which the ML estimate $\mathbf{x}_{\hat{m},\hat{n},\hat{u}}(t)$ is different from the actual data vector $\mathbf{x}_{m,n,u}(t)$. Based on the ML algorithm as depicted in (10), we have

$$E(\mathbf{x}_{m,n,u}(t), \mathbf{x}_{\hat{m},\hat{n},\hat{u}}(t)) = \|\mathbf{R} - \mathbf{H}\mathbf{X}_{m,n,u}\|_F^2 > \|\mathbf{R} - \mathbf{H}\mathbf{X}_{\hat{m},\hat{n},\hat{u}}\|_F^2 \quad (28)$$

Substituting (7) into (28), we have that a symbol error occurs when

$$\|\mathbf{V}\|_F^2 > \|\mathbf{H}(\mathbf{X}_{m,n,u} - \mathbf{X}_{\hat{m},\hat{n},\hat{u}}) + \mathbf{V}\|_F^2 \quad (29)$$

Let $\mathbf{C} \equiv \mathbf{X}_{m,n,u} - \mathbf{X}_{\hat{m},\hat{n},\hat{u}}$ and exploit the fact that $\|\mathbf{A}\|_F^2 = \text{tr}(\mathbf{A}^T \mathbf{A})$, (29) can be reformulated as

$$-\text{tr}(\mathbf{C}^T \mathbf{H}^T \mathbf{V}) > \frac{1}{2} \|\mathbf{H}\mathbf{C}\|_F^2 \quad (30)$$

Let random variable Z be defined as $Z \equiv -\text{tr}(\mathbf{C}^T \mathbf{H}^T \mathbf{V})$, we can derive that $Z \sim N(0, \sigma^2 \|\mathbf{H}\mathbf{C}\|_F^2)$. Therefore, the PEP of transmitting $\mathbf{x}_{m,n,u}(t)$ and erroneously detecting as $\mathbf{x}_{\hat{m},\hat{n},\hat{u}}(t)$ can be calculated as

$$P_e(\mathbf{x}_{m,n,u}(t) \rightarrow \mathbf{x}_{\hat{m},\hat{n},\hat{u}}(t)) = P\left(Z > \frac{1}{2} \|\mathbf{H}\mathbf{C}\|_F^2\right) = Q\left(\frac{\|\mathbf{H}\mathbf{C}\|_F}{2\sigma}\right) \quad (31)$$

Substituting (31) into (27), the upper bound of $P_{e,ML}$ can be obtained.

4.2 SER of the proposed algorithm

Let $P_{e,u}$ be the SER when the u th LED is selected to transmit information, then under equal a priori probability assumption, the average overall SER can be expressed as

$$P_e = \frac{1}{N_t} \sum_{u=1}^{N_t} P_{e,u} \quad (32)$$

Let $P_{e,s|u}$, $P_{e,MPAM|u}$, $P_{e,NPWM|u}$ denote the probability of making error decision of spatial symbol, MPAM and NPWM temporal symbols, respectively. We may separate the error types of $P_{e,u}$ into the following parts:

- (a) Active LED is erroneously detected (spatial symbol error); both MPAM and NPWM temporal symbols are error.
- (b) Both spatial and MPAM symbols are error, while NPWM symbols are correct.
- (c) Both spatial and NPWM symbols are error, while MPAM symbols are correct.
- (d) Spatial symbol is error, while both temporal symbols are correct.
- (e) Spatial symbol is correct, while both temporal symbols are error.
- (f) Spatial and NPWM symbols are correct, while MPAM symbol is error.
- (g) Spatial and MPAM symbols are correct, while NPWM symbol is error.

In what follows, we have

$$\begin{aligned}
 P_{e,u} &= P_{e,s|u} P_{e,MPAM|u} P_{e,NPWM|u} + P_{e,s|u} P_{e,MPAM|u} (1 - P_{e,NPWM|u}) \\
 &\quad + P_{e,s|u} (1 - P_{e,MPAM|u}) P_{e,NPWM|u} + P_{e,s|u} (1 - P_{e,MPAM|u}) (1 - P_{e,NPWM|u}) \\
 &\quad + (1 - P_{e,s|u}) P_{e,MPAM|u} P_{e,NPWM|u} + (1 - P_{e,s|u}) P_{e,MPAM|u} (1 - P_{e,NPWM|u}) \\
 &\quad + (1 - P_{e,s|u}) (1 - P_{e,MPAM|u}) P_{e,NPWM|u} \\
 &= P_{e,s|u} + (1 - P_{e,s|u}) (P_{e,MPAM|u} + P_{e,NPWM|u} - P_{e,MPAM|u} P_{e,NPWM|u})
 \end{aligned} \tag{33}$$

At high SNR, the term $P_{e,MPAM|u} P_{e,NPWM|u}$ is usually small compared with the other terms and thus can be neglected. Hence, (33) can be approximately as

$$P_{e,u} \approx P_{e,s|u} + (1 - P_{e,s|u}) (P_{e,MPAM|u} + P_{e,NPWM|u}) \tag{34}$$

To derive $P_{e,s|u}$, we should base on the spatial symbol detection algorithm as described in Sect. 3.2.1. Given that u th LED is activated and the symbol being $s_{m,n}(t)$, the correct detection probability of activated LED can be derived as

$$\begin{aligned}
 P_{c,s|u,s_{m,n}(t)} &= P(\mathbf{y}_1(u) > \max \{ \mathbf{y}_1(1), \dots, \mathbf{y}_1(u-1), \mathbf{y}_1(u+1), \dots, \mathbf{y}_1(N_t) \} | s_{m,n}(t)) \\
 &= P(\mathbf{y}_1(u) > \mathbf{y}_1(1), \mathbf{y}_1(u) > \mathbf{y}_1(2), \dots, \mathbf{y}_1(u) > \mathbf{y}_1(N_t) | s_{m,n}(t)) \\
 &= \int_{-\infty}^{\infty} f_{\mathbf{y}_1(u)}(t | s_{m,n}(t)) \prod_{\substack{i=1 \\ i \neq u}}^{N_t} P(\mathbf{y}_1(i) < t | s_{m,n}(t)) dt \\
 &= \int_{-\infty}^{\infty} \prod_{\substack{i=1 \\ i \neq u}}^{N_t} \left[1 - Q\left(\frac{t - \alpha_{iu} \frac{\|\mathbf{h}_u\| P_t m n \tau}{M}}{\sigma \sqrt{N \tau}} \right) \right] \frac{1}{\sqrt{2\pi N \tau} \sigma} \exp\left(-\frac{\left(t - \frac{\|\mathbf{h}_u\| P_t m n \tau}{M} \right)^2}{2\sigma^2 N \tau} \right) dt
 \end{aligned} \tag{35}$$

Under equal a priori probability assumption, the average correct detection probability of active LED can then be obtained as

$$P_{c,s|u} = \frac{1}{MN} \sum_{m=1}^M \sum_{n=1}^N P_{c,s|u,s_{m,n}(t)} \tag{36}$$

Therefore

$$P_{e,s|u} = 1 - P_{c,s|u} = 1 - \frac{1}{MN} \sum_{m=1}^M \sum_{n=1}^N P_{c,s|u,s_{m,n}(t)} \tag{37}$$

Based on the decision rule of (22), the average SER of M -ary PAM can be derived as

$$\begin{aligned}
 P_{e,MPAM|u} &= \sum_{m=1}^M P\left(\hat{m} \neq m | s_{m,n}(t) = \frac{m P_t}{M} p_{\tau}(t) \right) P\left(s_{m,n}(t) = \frac{m P_t}{M} p_{\tau}(t) \right) \\
 &= \frac{1}{M} \left[Q\left(\frac{d_{u,2}}{2\sigma \sqrt{\tau}} \right) + 2(M-2) Q\left(\frac{d_{u,2}}{2\sigma \sqrt{\tau}} \right) + Q\left(\frac{d_{u,2}}{2\sigma \sqrt{\tau}} \right) \right] \\
 &= \frac{2(M-1)}{M} Q\left(\frac{d_{u,2}}{2\sigma \sqrt{\tau}} \right) \\
 &= \frac{2(M-1)}{M} Q\left(\frac{\|\mathbf{h}_u\| P_t \sqrt{\tau}}{2\sigma M} \right)
 \end{aligned} \tag{38}$$

Similarly, according to the decision rule of (26), the average SER of N -ary PWM can be derived as

$$\begin{aligned}
 P_{e, \text{NPWM} | u} &= \sum_{n=1}^N \sum_{m=1}^M P\left(\hat{n} \neq n | s_{m,n}(t) = \frac{mP_t}{M} p_{n\tau}(t)\right) P\left(s_{m,n}(t) = \frac{mP_t}{M} p_{n\tau}(t)\right) \\
 &= \frac{1}{NM} \left[Q\left(\frac{d_{u,1}}{2\sigma\sqrt{N\tau}}\right) + 2(M-2)Q\left(\frac{d_{u,1}}{2\sigma\sqrt{N\tau}}\right) + Q\left(\frac{d_{u,1}}{2\sigma\sqrt{N\tau}}\right) \right] \\
 &= \frac{2(N-1)}{NM} \sum_{m=1}^M Q\left(\frac{d_{u,1}}{2\sigma\sqrt{N\tau}}\right) \\
 &= \frac{2(N-1)}{NM} \sum_{m=1}^M Q\left(\frac{\|\mathbf{h}_u\|P_t m\sqrt{\tau}}{2\sigma M\sqrt{N}}\right)
 \end{aligned} \tag{39}$$

Toward this end, $P_{e,u}$ can then be obtained by substituting (37)–(39) into (34).

$$\begin{aligned}
 P_{e,u} &= 1 - \frac{1}{MN} \sum_{m=1}^M \sum_{n=1}^N P_{c,s|u,s_{m,n}(t)} \\
 &+ \left(\frac{1}{MN} \sum_{m=1}^M \sum_{n=1}^N P_{c,s|u,s_{m,n}(t)} \right) \\
 &\times \left[\frac{2(M-1)}{M} Q\left(\frac{\|\mathbf{h}_u\|P_t\sqrt{\tau}}{2\sigma M}\right) + \frac{2(N-1)}{NM} \sum_{m=1}^M Q\left(\frac{\|\mathbf{h}_u\|P_t m\sqrt{\tau}}{2\sigma M\sqrt{N}}\right) \right]
 \end{aligned} \tag{40}$$

Finally substituting (40) into (32), the theoretical expression of the average SER of the proposed scheme can be derived.

5 Results and discussion

5.1 Complexity analysis

In this subsection, we evaluate and compare the complexity of the proposed MF-based scheme with the ML detector. The computation load is measured using the total number of floating-point operations (flops) [22] required at the SM receiver, *e.g.*, one flop is carried out for real addition and multiplication. Therefore, the multiplication of $m \times n$ and $n \times p$ real matrices requires $m \times n \times p$ flops.

Based on the ML algorithm as depicted in (10), we can obtain that the number of flops required to implement the ML detector is $MNN_t(N_r N_t N + N^2 N_r)$ flops (in which totally MNN_t trials required with $N_r N_t N + N^2 N_r$ flops for each trial). Alternatively, as depicted in Eqs. (13–14, 17), only $N_t N_r + N_t N$ flops are required to realize the proposed algorithm. Taking a general parameters' setting as a working example: $N_r = 10, N_t = 8, M = 16, N = 8$, the number of flops required for the proposed, and ML algorithms are 144 and 1,310,720, respectively. It is shown that the computation load of the proposed algorithm is extensively reduced compared to the ML algorithm.

5.2 Performance comparison of the ML and proposed detection algorithms

In this subsection, we will validate the theoretical derivation in previous section by computer simulation. Moreover, we will compare the performance of the optimum

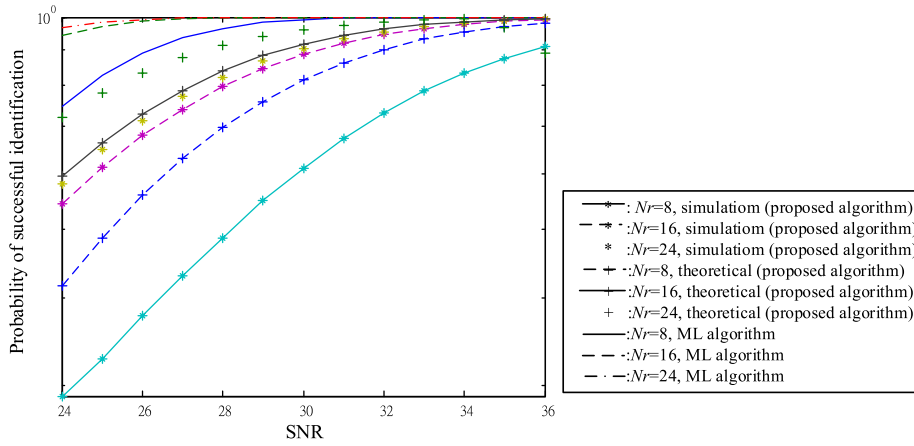


Fig. 4 Probability of successful identification of the activated LED with respect to SNR, where $(N_r, M, N) = (8, 4, 8)$

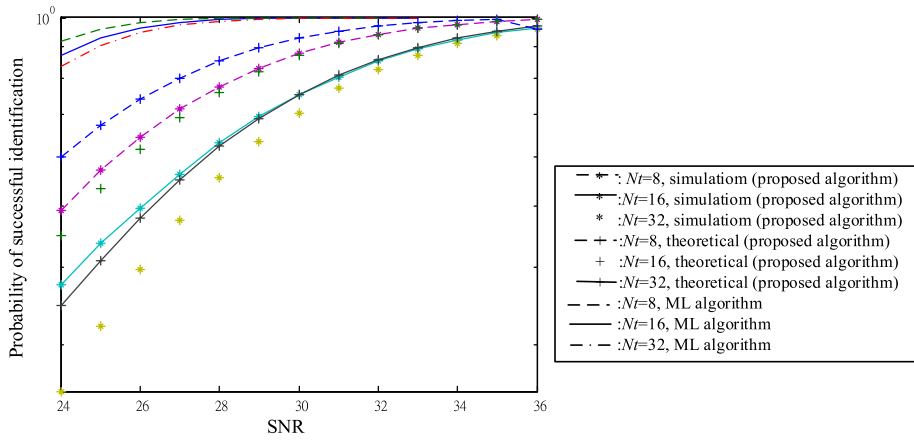


Fig. 5 Probability of successful identification of the activated LED with respect to SNR, where $(N_r, M, N) = (12, 4, 8)$

ML and the proposed detection scheme. The parameters setting of the indoor MIMO VLC channel follow those parameters given in [22]: $\eta = 0.53$, $\phi_{1/2} = 37.5^\circ$, $\Psi_{1/2} = 90^\circ$, $A = 50 \text{ mm}^2$, and d_{ij} is set to be uniformly distributed within $2 \sim 3 \text{ m}$. Note that the signal-to-noise power ratio (SNR) exploited for simulation is defined as $\text{SNR} = 10 \log_{10} \frac{P_t}{\sigma^2} \text{ (dB)}$ and the simulation result is obtained from the average of 100,000 independent trials.

Since identification of the index of active LED at the transmitter is essential for the proposed algorithm, hence, we aim to evaluate the performance of the correct identification probability of the proposed algorithm. Figure 4 presents the simulation and theoretical [we use (35) and (36) to evaluate $P_{c,s|u}$] results of the probability of successful identification with respect to SNR, where the spatial-temporal modulation order is set as $(N_t, M, N) = (8, 4, 8)$, respectively. The scenarios for different receiver array size, $N_r = 8, 16, 24$, are provided for comparison. Alternatively, we fix the receiver array size as $N_r = 12$, and the results for different spatial modulation order

$N_t = 8, 16, 32$ are presented in Fig. 5. From the results depicted in Figs. 4 and 5, we have the following observations:

- (1) As SNR increases, the correct identification probability of the index of activated LED increases as well.
- (2) Theoretical results are slightly better than the simulation results, whereas ML detection significantly outperforms the proposed detection algorithm. Nevertheless, as described in the previous subsection, the price for ML algorithm is higher and thus impractical computation load.
- (3) Performance degrades for larger N_t . It is as expected since it is more probable to misidentify the index of the activated LED for larger N_t . On the other hand, larger N_r leads to better performance. This is due mainly to the fact that as receive array size increases, larger degrees of freedom enhance the separability of the active LED from the inactive ones.

In the second part of simulations, we aim to evaluate the overall average SER ($P((u, m, n) \neq (\hat{u}, \hat{m}, \hat{n}); u, \hat{u} = 1, \dots, N_t, m, \hat{m} = 1, \dots, M, n, \hat{n} = 1, \dots, N)$) of the optimal ML and the proposed detection algorithms. Moreover, the performances of simulation and theoretical [we use (40), (35) and (32) to evaluate P_e] results of the proposed algorithm are also provided for comparison. As we set $(N_t, M, N) = (8, 4, 8)$, Fig. 6 presents the overall SER with respect to SNR for the cases of $N_r = 8, 16$, and 24, respectively, while in Fig. 7, we set $(N_r, M, N) = (12, 4, 8)$ and evaluate the overall SER for $N_t = 8, 16, 32$. Based on the results depicted in Figs. 6 and 7, we have

- (1) Figures 6 and 7 demonstrate that the ML detector outperforms the proposed detection scheme. However, the benefits of the proposed algorithm are that the complexity reduction overwhelms slightly degradation in SER performance.
- (2) Figures 6 and 7 verify that the SER performance of the theoretical and computer simulation results is in good agreement.

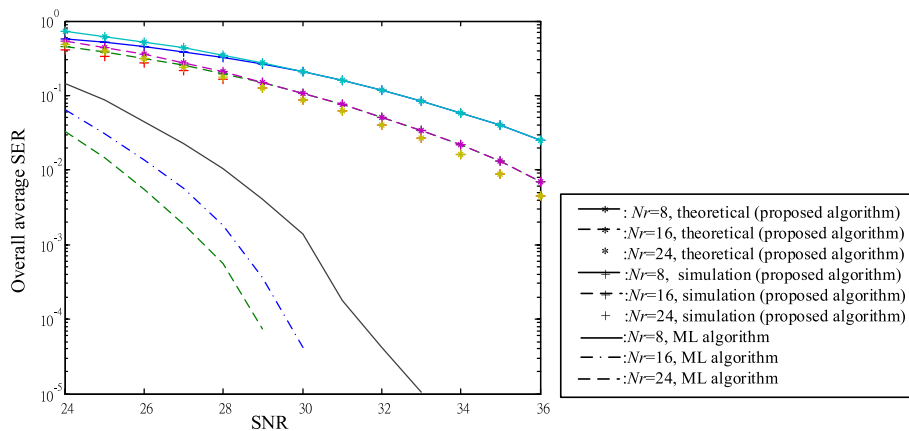


Fig. 6 Overall average SER with respect to SNR, where $(N_t, M, N) = (8, 4, 8)$

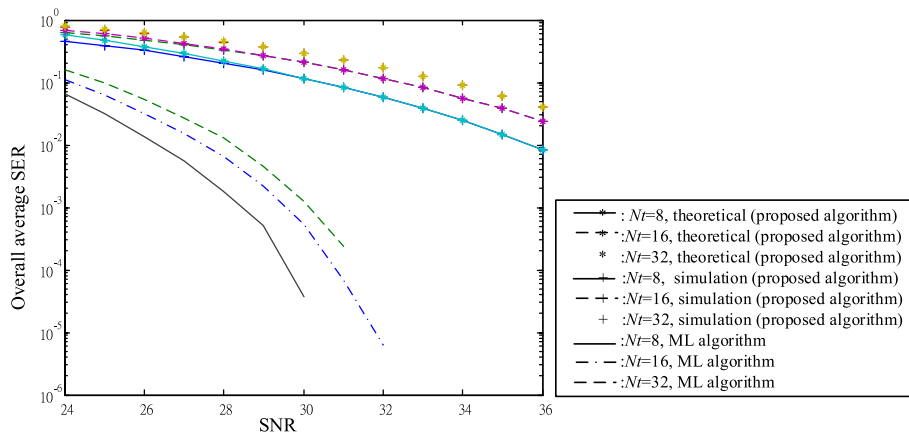


Fig. 7 Overall average SER with respect to SNR, where $(N_r, M, N) = (12, 4, 8)$

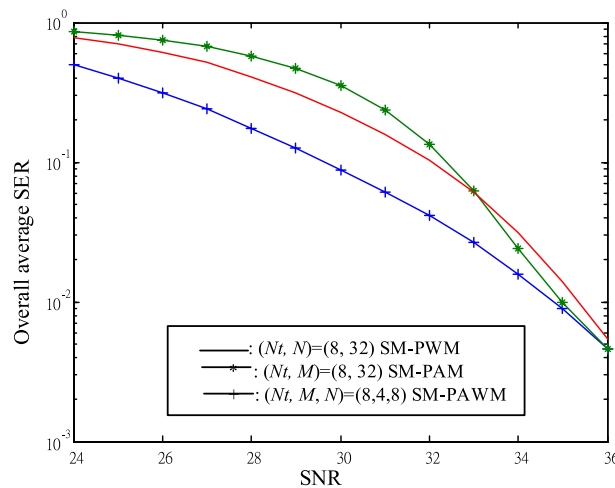


Fig. 8 Overall average SER with respect to SNR for SM-PAWM, SM-PWM, and SM-PAM systems

(3) Figures 6 and 7, respectively, demonstrate that larger N_r and/or smaller N_t yields better SER performance. The reasons are as we have claimed that as N_r is large, the spatial signatures of $\{\mathbf{h}_i\}_{i=1, \dots, N_t}$ are more separable and larger N_t corresponds to larger spatial SER.

Finally, we compare the overall SER performance between the proposed SM-PAWM and conventional optical spatial modulations, such as SM-PAM or SM-PWM. To make the comparison fair, the SER of the three schemes should be evaluated under the same bpcu. For example, a $(N_t, M, N)=(8, 4, 8)$ SM-PAWM system should be compared with $(N_t, M) = (8, 32)$ SM-PAM or $(N_t, N) = (8, 32)$ SM-PWM system since their bpcu are all equal to 8 ($\eta = \log_2 8 + \log_2 4 + \log_2 8 = \log_2 8 + \log_2 32 = 8$). Figure 8 presents the overall SER with respect to SNR for the $(N_t, M, N)=(8, 4, 8)$ SM-PAWM, $(N_t, M) = (8, 32)$ SM-PAM, and $(N_t, N) = (8, 32)$ SM-PWM systems in

which the number of PDs at the receiving end is set as $N_r = 16$. As verified by the results presented in the figure, the proposed SM-PAWM scheme outperforms the conventional SM-PAM and SM-PWM schemes.

6 Conclusions

In this paper, we have proposed a novel optical modulation and signaling scheme, named SM-PAWM, operating in VLC MIMO communication system. The proposed SM-PAWM scheme has higher spectral efficiency or bpcu over conventional SM based optical communication systems. Moreover, we have developed a novel detection scheme that are computationally efficient compared to the existing optimum ML detector. The theoretical analysis of the overall average SER has been comprehensively derived. Through extensive computer simulations, we have verified that the analytical and numerical results of the proposed algorithm are closely matched. It has been verified that the proposed detector can work reliably in VLC MIMO channel as the number of receiver array size is large and/or the number of LEDs is small. Therefore, with a much lower computational complexity, the proposed detection scheme is a feasible alternative to the existing ML detector for SM MIMO VLC system.

Abbreviations

VLC	Visible light communication
SM	Spatial modulation
MIMO	Multi-input multi-output
SMF	Spatial matched filtering
PAWM	Pulse amplitude Width Modulation
LED	Light-emitting diodes
bpcu	Bits per channel use
ML	Maximum likelihood
SER	Symbol error rate
PD	Photodetector
PAM	Pulse amplitude modulation
AWGN	Additive white Gaussian noise

Author contributions

The author W-CW is responsible for the following: conceptualization, methodology, software, data curation, writing—original draft preparation, investigation, software, validation, writing—reviewing and editing.

Funding

The authors declare that they have no Funding.

Data availability

The data that support the findings of this study are available on request from the corresponding author.

Declarations

Competing interests

The authors declare that they have no Competing interests.

Received: 11 January 2023 Accepted: 8 February 2024

Published online: 13 February 2024

References

1. R. Mesleh, A. Alhassi, *Space Modulation Techniques* (Wiley, Hoboken, 2018)
2. R.Y. Mesleh, H. Haas et al., Spatial modulation. *IEEE Trans. Vehic. Technol.* **57**(4), 2228–2241 (2008). <https://doi.org/10.1109/TVT.2007.912136>
3. R. Y. Mesleh, H. Haas, C. W. Ahn, and S. Yun. Spatial modulation—a new low complexity spectral efficiency enhancing technique, in *Proceedings IEEE International Conference Communication Network* (China, 2006), pp. 1–5. <https://doi.org/10.1109/CHINACOM.2006.344658>

4. M.D. Renzo, H. Haas, P.M. Grant, Spatial modulation for multiple antenna wireless systems—a survey. *IEEE Commun. Mag.* **49**(12), 182–191 (2011). <https://doi.org/10.1109/MCOM.2011.6094024>
5. K.M. Humadi, A.I. Sulyman, A. Alsanie, Spatial modulation concept for massive multiuser MIMO systems. *Int. J. Antenn. Propagat.* **1**, 1–9 (2014). <https://doi.org/10.1155/2014/563273>
6. T. Fath, M. D. Renzo, and H. Haas. On the performance of space shift keying for optical wireless communications, in *Proceedings IEEE Global Communication Conference—Workshop Optical Wireless Communication*, (Miami, FL, USA, 2010), pp. 990–994. <https://doi.org/10.1109/GLOCOMW.2010.5700474>
7. R. Mesleh, H. Elgala, H. Haas, Optical spatial modulation. *J. Optic. Commun. Network.* **3**(3), 234–244 (2011). <https://doi.org/10.1364/JOCN.3.000234>
8. R. Mesleh, H. Elgala, R. Mehmood, H. Haas, Performance of optical spatial modulation with transmitters-receivers alignment. *IEEE Commun. Lett.* **15**(1), 79–81 (2011). <https://doi.org/10.1109/LCOMM.2010.01.101208>
9. W. Popoola, E. Poves, H. Haas, Spatial pulse position modulation for optical communications. *J. Lightwave Technol.* **30**(18), 2948–2954 (2012). <https://doi.org/10.1109/JLT.2012.2208940>
10. T. Fath, H. Haas, M. Di Renzo, and R. Mesleh. Spatial modulation applied to optical wireless communications in indoor LoS environments, in *Proceedings IEEE Global Telecommunication Conference*, (Houston, TX, USA, 2011), pp. 1–5. <https://doi.org/10.1109/GLOCOM.2011.6133552>
11. C.R. Kumar, R.K. Jeyachitra, Improved joint generalized spatial modulations for MIMO-VLC systems. *IEEE Commun. Lett.* **22**(11), 2226–2229 (2018). <https://doi.org/10.1109/LCOMM.2018.2868189>
12. S. P. Alaka, T. L. Narasimhan, and A. Chockalingam. Generalized spatial modulation in indoor wireless visible light communication, in *Proceedings IEEE Global Communication Conference*, (San Diego, CA, USA, 2015), pp. 1–7. <https://doi.org/10.1109/GLOCOM.2014.7416970>
13. A. Stavridis and H. Haas. Performance evaluation of space modulation techniques in VLC systems, in *Proceedings IEEE International Conference Communication Workshops (ICC)*, (London, UK, 2015), pp. 1356–1361. <https://doi.org/10.1109/ICCW.2015.7247367>
14. W.O. Popoola, H. Haas, Demonstration of the merit and limitation of generalised space shift keying for indoor visible light communications. *J. Lightwave Technol.* **32**(10), 1960–1965 (2014). <https://doi.org/10.1109/JLT.2014.2310499>
15. J.Y. Wang, J.X. Zhu, S.H. Lin, J.B. Wang, Adaptive spatial modulation based visible light communications: SER analysis and optimization. *IEEE Photon. J.* (2018). <https://doi.org/10.1109/JPHOT.2018.2834388>
16. W. Popoola, E. Poves, H. Haas, Error performance of generalized space shift keying for indoor visible light communications. *IEEE Trans. Commun.* **61**(5), 1968–1976 (2013). <https://doi.org/10.1109/TCOMM.2013.022713.120501>
17. R. Mesleh, R. Mehmood, H. Elgala, and H. Haas. Indoor MIMO optical wireless communication using spatial modulation, in *Proceedings IEEE International Conference Communication*, (Cape Town, South Africa, 2010), pp. 1–5. <https://doi.org/10.1109/ICC.2010.5502062>
18. M.D. Renzo, H. Hass, A. Ghayeb, S. Sugiura, Spatial modulation for generalized MIMO: challenges, opportunities and implementation. *Proc. IEEE* **102**(1), 56–103 (2014). <https://doi.org/10.1109/JPROC.2013.2287851>
19. J.M. Kahn, J.R. Barry, Wireless infrared communications. *Proc. IEEE* **85**(2), 265–298 (1997). <https://doi.org/10.1109/5.554222>
20. T. Fath, H. Haas, Performance comparison of MIMO techniques for optical wireless communications in indoor environments. *IEEE Trans. Commun.* **61**(2), 733–742 (2013). <https://doi.org/10.1109/TCOMM.2012.120512.110578>
21. J.-Y. Wang, J. Dai, R. Guan, L. Jia, Y. Wang, M. Chen, On the channel capacity and receiver deployment optimization for multi-input multi-output visible light communications. *Opt. Express* **24**(12), 13060–13074 (2016). <https://doi.org/10.1364/OE.24.013060>
22. E. Curry, D.K. Borah, Iterative combinatorial symbol design for spatial modulations in MIMO VLC systems. *IEEE Photonic Technol. Lett.* **30**(5), 483–486 (2018). <https://doi.org/10.1109/LPT.2018.2797130>

Publisher's Note

Springer Nature remains neutral with regard to jurisdictional claims in published maps and institutional affiliations.